In Situ Deployment of Voltammetric, Potentiometric, and Amperometric Microelectrodes from a ROV To Determine Dissolved O 2 , Mn, Fe, S(−2), and pH in Porewaters

ARTICLE *in* ENVIRONMENTAL SCIENCE AND TECHNOLOGY · DECEMBER 1999

Impact Factor: 5.33 · DOI: 10.1021/es9904991

4 AUTHORS, INCLUDING:

George W Luther
University of Delaware
316 PUBLICATIONS **12,896** CITATIONS
SEE PROFILE

Clare Reimers
Oregon State University
87 PUBLICATIONS **4,714** CITATIONS
SEE PROFILE

Donald B. Nuzzio
Analytical Instrument Systems, Inc.
37 PUBLICATIONS **1,092** CITATIONS
SEE PROFILE

Environ. Sci. Technol. **1999**, *33,* 4352−4356

In Situ Deployment of Voltammetric, Potentiometric, and Amperometric Microelectrodes from a ROV To Determine Dissolved O_2, Mn, Fe, S(−2), and pH in Porewaters

GEORGE W. LUTHER, III*
College of Marine Studies, University of Delaware, Lewes, Delaware 19958

CLARE E. REIMERS
Institute of Marine and Coastal Sciences, Rutgers University, New Brunswick, New Jersey 08901-8521

DONALD B. NUZZIO
Analytical Instrument Systems, Inc., Flemington, New Jersey 08822-0458

DAVID LOVALVO
Eastern Oceanics, Inc., West Redding, Connecticut 06896

Solid-state microelectrodes have been used in situ in Raritan Bay, NJ to measure pore water profiles of dissolved O_2, Mn, Fe, and sulfide at (sub)millimeter resolution by voltammetric techniques. The voltammetric sensor was positioned with microprofiling instrumentation mounted on a small remote operated vehicle (ROV). This instrumentation and the sensor were controlled and monitored in real time from a research vessel anchored at the study site. The voltammetric analyzer was connected to the electrodes of the voltammetric cell with a 30 m cable which also bridged receiver-transmitter transducers to ensure signal quality along the cable. Single analyte O_2, pH, and resistivity microsensors were operated alongside the voltammetric sensor. We report on the technology of the system and the concentration changes of redox species observed from 2 to 3 cm above to approximately 4 cm below the sediment−water interface during three deployments. O_2 measurements from both Clark and voltammetric electrodes were in excellent agreement. The profiles obtained show that there is no detectable overlap of O_2 and Mn^{2+} in the sediments which is similar to previous reports from other continental margin sediments which were cored and analyzed in the laboratory. These data indicate that O_2 is not a direct oxidant for Mn^{2+} when diffusive (rather than advective) processes control the transport of solutes within the sediment. Subsurface Mn^{2+} peaks were observed at about 2 cm and coincide with a subsurface pH maximum. The data can be explained by organic matter decomposition with alternate electron acceptors and by the formation of authigenic phases containing reduced Mn at depth.

Introduction

The determination of the major dissolved redox species (O_2, Mn, Fe, and S(−2)) found in sedimentary environments using voltammetry at a gold-amalgam (Au/Hg) electrode was reported by Brendel and Luther (*1*). For this earlier work, marine sediment cores were retrieved and analyzed aboard ship or in the laboratory. In this paper we report the use of Au/Hg electrodes to determine these species in situ, in real time, and in profiles with (sub)millimeter resolution (microprofiles). The voltammetric electrodes were mounted on microprofiling instruments attached to a remote operated vehicle (ROV) along with pH microelectrodes, Clark-style O_2 microelectrodes, and a resistivity sensor. A portable dc powered voltammetric analyzer with a 30 m cable between it, sender/transmitter units, and the electrodes of the voltammetric cell facilitated the real-time voltammetric analysis. Video cameras on the ROV permitted observation of the sensors. Real-time operation and observation have many advantages for measuring detailed chemical distributions at the seafloor. First, the operator knows immediately if there are equipment problems, so the ROV can be recovered, saving valuable field time. Second, microprofiles may be started, run, or stopped exactly at distances desired, rather than by a preprogrammed, hit-or-miss approach. Third, voltammetric measurements may be improved by varying electrochemical conditioning steps and scanning parameters in response to observed signals.

Redox species and pH are telling parameters for separating the competing chemical and biochemical reactions that mediate organic matter decomposition and mineral dissolution/precipitation in surface sediments (*2*−*5*). For example, it is often assumed that species such as O_2 may be consumed in pore waters both as an organic matter oxidant and as an oxidant of reduced metabolites transported upward toward the sediment−water interface. In this paper, we show that (1) there is no overlap of the Mn^{2+} and O_2 profiles and that (2) changes in the pH profiles correlate with Mn^{2+} and O_2 changes. We describe possible reactions that can cause these porewater distributions. We also describe the technical fine points of our in situ measurements.

Experimental Section

Study Area and Dives. The area studied was within Raritan Bay, NJ (∼40°27.5 N; 74°04.5 W; water depth 6−7 m; June 27−30, 1997). The three ROV dives from which measurements are reported took place during afternoon or evening hours and lasted from 1.3 to 2.5 h. A CTD mounted on the ROV indicated that the salinity of the bottom water ranged from 26.4 to 26.9 and the water temperature ranged from 20.0 to 20.6 °C during the dives. The sediments were fine-grained with organic carbon contents of 3−4% but <1% carbonate carbon. Formation factor profiles indicate that porosities decreased to ∼0.82 over the first centimeter of depth and then remained >0.75 to at least 4 cm.

Field Instrumentation. The **ROV** (Eastern Oceanics, Inc) used in this project was designed for work at water depths less than 300 m. The ROV carries a forward-looking color video camera with tilt and pan controls, lights, an adjustable ballast system, and a framework of high-strength aluminum "Speed-Rail" (Hollander, Inc.). The Speed-Rail allows easy attachment of instruments. The instruments attached during this work were two microprofilers, a transmitter unit and separate cable for boosting the signals from the voltammetric sensor, a coring system, a CTD, a Niskin bottle, and two additional video cameras for close-up viewing of all the microelectrodes (pH, Clark, and voltammetric).

Microprofilers support microelectrodes and measure fine-scale chemical profiles centered at the sediment−water interface. Since their inception by Reimers (*5*), these units

* Corresponding author phone: (302)645-4208; fax: (302)645-4007; e-mail: luther@Udel.edu.

10.1021/es9904991 CCC: $18.00
Published on Web 10/21/1999

have consisted of a cylindrical pressure housing containing the unit's controller (currently a *Tattletale 2B, Onset Computers)*, analogue signal processing boards, and batteries, with microelectrodes mounted to the bottom end cap and a drive motor assembly mounted either on top of the main housing or off to the side. To optimize the operation of two microprofilers on a small ROV (one for measuring O_2 and resistivity, and another for pH and voltammetry), we modified the design so that smaller and lighter packages are moved up and down during profiling. This was accomplished by building profiling units that consist only of a motor, lead screw, cam and switch (for counting individual 0.25 mm vertical steps), and a support ring for mounting the microelectrodes. These units are mounted at the front end of the ROV in view of the main video camera, on motorized slides. Each slide has controls to raise and lower the microprofiling units rapidly over ~20 cm that are independent of the profiler's electronics for fine-scale travel. Cabling is used to connect the separated sensors and motor/switch to each unit's electronics housing, and the housings are clamped to the Speed-Rail frame of the ROV near its center of mass. Cables are also run from each housing to join with the ROV's tether and an RS-232-interface so that the microprofilers can be operated in real-time.

Microelectrodes and Analytical Methods. *Single Analyte Sensors.* Clark-style O_2 microelectrodes, pH microelectrodes, and resistivity sensors were made and applied following methods similar to those described by Revsbech and Jørgensen *(6)*, Cai and Reimers *(7)*, and Andrews and Bennett *(8)*. For all dives, four Clark-style sensors and one resistivity sensor were mounted on one microprofiler, while two or three pH microelectrodes, a pH reference electrode (Ag/AgCl), and the three electrodes of the voltammetric cell (see below) were attached to the second microprofiler. The first profiler was programmed to wait for several initialization commands and then to lower and read the O_2 microelectrodes and resistivity sensor every 0.25 mm at a set time (~10 s) over the length of a profile. In contrast, the timing and step size of the vertical movement for the second profiler was controlled by the analyst via computer to allow for real-time acquisition and electrochemical experimentation when necessary.

Voltammetric Sensors. Two types of voltammetric microelectrodes were constructed for this study.

(1) **Gold amalgam glass electrodes** were constructed as described in Brendel and Luther *(1)* with modifications to ensure a waterproof seal. Briefly, the end of a 15 cm section of 4 mm-diameter glass tubing was heated in a small flame and the tip pulled to a diameter of less than 0.4 mm for a length of about 3−5 cm. A 100-μm diameter gold wire was then inserted, and the tip was placed back into the flame to seal the gold into the glass. Once cooled the excess glass was sanded away with 400 grit sandpaper on a polisher to expose the gold wire. The copper conducting wire of a BNC cable was epoxied with a silver epoxy (Epotek H20-E) to the gold wire inside the glass. The electrode was then filled with Fluorinert (3M Inc.) and sealed at the top of the glass with heat shrink tubing. Then, the top end was coated with Scotchkote (3M) electrical coating and Scotchfil (3M) electrical insulation putty which makes a waterproof seal.

Alternately, a nonconductive epoxy was used as a fill. In this work, we used West System 105 epoxy resin and 206 hardener to form a high-purity, optical-grade, nonconductive fill. The epoxy was injected into the glass which contained the gold wire that was previously soldered to the conductor wire of the BNC cable but which was not sealed at the tip. The epoxy has a moderate setting time (~1 h) and drains slowly through the open tip. On setting, the epoxy seals the tip and the top end can be refilled with epoxy. Then the top end is coated with Scotchkote (3M) electrical coating and Scotchfil (3M) electrical insulation putty. After final setting of the epoxy, the tip is sanded and polished. We have tested this design in the lab at a pressure of 200 atm without failures.

(2) **Gold amalgam PEEK electrodes** were made by fixing 100-μm diameter Au wire soldered to the conductor wire of BNC cable within a body of 0.125" diameter PEEK tubing, which is commercially available as standard HPLC high-pressure tubing. The metal is fixed within the tubing with the West System 105 epoxy resin and 206 hardener as described above. PEEK and high-purity epoxy fill permits the determination of metal concentrations without risk of contamination and at temperatures as high as 115 °C.

Once constructed each electrode surface was polished and plated with Hg by reducing Hg(II) from a 0.1 N Hg/0.05 N HNO_3 solution, for 4 min at a potential of −0.1 V, while purging with N_2. The mercury/gold amalgam interface was conditioned using a 90 s−9 V polarization procedure in a 1 N NaOH solution (*1*). The electrode was then run in linear sweep mode from −0.05 to −1.8 V versus a saturated calomel electrode (SCE) or Ag/AgCl electrode several times in oxygenated seawater to obtain a reproducible O_2 signal.

An interesting problem with obtaining data in nearshore environments is the presence of organisms such as crabs that can attack and possibly break the tips of fragile microelectrodes. This was a major hindrance for collecting complete pH microprofiles in this study but rarely eliminated the voltammetric sensors because the epoxy fill gave a more durable electrode.

In Situ Voltammetric Analyses. All voltammetric analyses were carried out in real time using an Analytical Instrument Systems, Inc. (AIS) DLK-100 electrochemical analyzer, controlled by a microcomputer aboard ship and using software provided by the manufacturer. The analyzer and computer were connected to separate dc power sources. A long cable receiver, AIS Model DLK-LCR-1, was connected directly to the analyzer as an interface with a 30 m waterproof cable. The cable contained three shielded wires [center conductor with shield] for the working (Au/Hg), reference (Ag/AgCl), and counter (Pt) electrodes as well as dc power (+15 V, −15 V) and ground. The other end of the cable was connected to a transmitter, AIS Model DLK-LCT-1, enclosed in a pressure housing, and mounted on the ROV. The transmitter was connected via 1 m lengths of shielded cable directly to the working, reference, and counter electrodes mounted on a microprofiler. The working electrode acted as the virtual ground for the system. This setup allows signals to be transmitted through 30 m of cable without signal degeneration. We typically used linear sweep voltammetry (200 mV/s) and square wave voltammetry (1 mV scan increment, 100 mV/s, 24 mV pulse) wave forms for the in situ analyses. Any other electrochemical waveform can also be applied to this electrode system. The potential range scanned was typically −0.05 to −1.8 V.

To maintain reproducibility during analysis, a conditioning step was used between each potential scan. When O_2 is present, conditioning is not necessary, and a value more negative than −0.1 V will result in partial consumption of O_2. We have found that a potential of −0.05 V for a period of <20 s restores the electrode surface while measuring Fe and/or Mn in anoxic environments when H_2S is not present. If H_2S or a soluble Fe(III) species is present, a potential of −0.8 V is used to remove any Fe, Mn, and sulfide deposited on the electrode, since none of these species is electroactive at this potential.

Standardization and Stability. The working voltammetric electrodes were standardized by placing filtered seawater in a polarographic cell and obtaining a curve with the desired standard over the range of concentrations expected in our samples. Table 1 gives data for typical calibration curves of each species including the minimum detection limits (MDL) which were determined by statistical comparison of blank

TABLE 1. Electrode Reactions at the Au/Hg Electrode vs the SCE and Calibration Data at 25 °C[a]

electrode reaction	E_p (V)	MDL (μM)	calibration slope (nA/μM)
$O_2 + 2H^+ + 2e^- \rightarrow H_2O_2$	−0.30	5	0.152
$H_2O_2 + 2H^+ + 2e^- \rightarrow 2H_2O$	−1.30	5	0.152
$HS^- + Hg \leftrightarrow HgS + H^+ + 2e^-$	−0.62	<0.2	2.2
$Fe^{2+} + Hg + 2e^- \leftrightarrow Fe(Hg)$	−1.43	10	0.025
$Mn^{2+} + Hg + 2e^- \leftrightarrow Mn(Hg)$	−1.55	3−5	0.070
$2I^- + 2Hg \leftrightarrow Hg_2I_2 + 2e^-$	−0.30	<0.2	3.2
$2S_2O_3^{2-} + Hg \leftrightarrow Hg(S_2O_3)_2^{2-} + 2e^-$	−0.15	16	0.111
$Fe^{3+} + e^- \rightarrow Fe^{2+}$	−0.25 to −0.9	molecular species	
$FeS + 2e^- + H^+ \rightarrow Fe(Hg) + HS^-$	−1.1	molecular species	

[a] All data were obtained with a 100 μm diameter electrode (area = 7.85×10^{-3} mm^2). O_2 and H_2O_2 data were collected by linear sweep voltammetry; all others were collected by square wave voltammetry. MDL is the minimum detection limit and is calculated as in refs *10* and *11* at the 99% confidence limit.

solutions with standard solutions in seawater (*10, 11*). Calibration curves usually consist of four standard addition points with three replicates for each standard addition. The slopes (nA/μM) of the standard curves are adjusted for any difference between the in situ temperature and the laboratory temperature according to how the diffusion coefficient (D) changes with temperature, since the current measured is proportional to $D^{0.5}$ (*10*). In this study, the water temperature had a narrow range of 20.0−20.6 °C. In a given day in the field, a standard curve for only one analyte, Mn^{2+}, was generated because Mn^{2+} is quite stable at seawater pH and is the easiest standard to prepare. We then used the "pilot ion method" (*11*) which relies on the verified fact that the sensitivity ratios for all the calibration curves remain constant. Precision of voltammetric measurements, defined as ±1 SD about the mean peak height, is frequently better than 5%. The error bars plotted in the figures represent this precision and in many instances are narrower than the symbols are wide.

Results and Discussion

Profiles for O_2 with both Clark-style microsensors and voltammetric electrodes operating were determined on three dives. The voltammetric sensor was run in linear sweep mode to determine O_2 because the O_2 reduction peak is irreversible and there is no enhancement of sensitivity using the square wave mode for irreversible electrode reactions. Figure 1 shows a comparison of O_2 measurements by one of the amperometric Clark-style O_2 microsensors and the voltammetric microelectrode on ROV dive 6 (made on June 27, 1997). The intercomparison of the two techniques is excellent even though they entered the sediment at different locations. Two other dives (dives 11 and 12; June 30, 1997) showed similar results, although one profile from the Clark-style microsensors showed O_2 penetration to 6 mm depth, presumably due to biological disturbance of the sediment.

Profiles of O_2, Mn^{2+}, Fe^{2+}, and total H_2S [sum of H_2S, HS^-, and any S (−2 and 0) in polysulfide species, S_x^{2-}] were measured successfully with voltammetric sensors on three dives (dives 6, 11, 12). Figure 2 shows square wave voltammetric scans that were acquired over several depths in the profile from dive 11. The baseline is flat and reproducible and shows no significant noise for all scans. The major peak is due to Mn^{2+} at −1.46 V vs Ag/AgCl, and the current (concentration) increases as the Au/Hg electrode is inserted deeper into the sediment. The small broad peak at −0.52 V vs Ag/AgCl is due to an Fe(III) organic species (*12, 13*).

On only one dive were both reliable pH and voltammetric data obtained during this cruise (dive 11, Figure 3). Sulfide was detected and increased to about 4 μM at 40 mm depth only on dive 12 (Figure 4). Fe(III) species and thiosulfate were detected at a few different depths but are not plotted. The profiles in Figures 3 and 4 show the same trends for

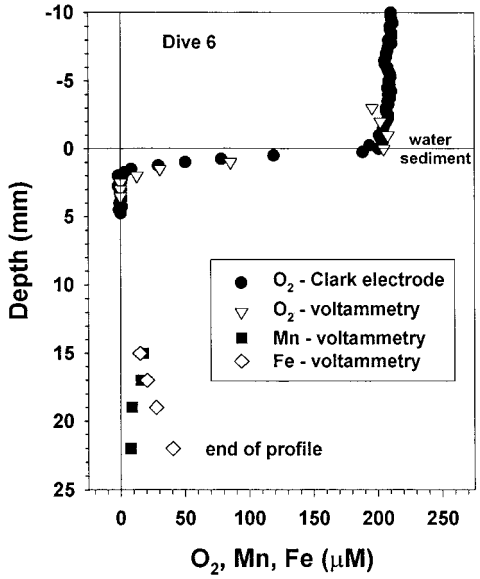

FIGURE 1. In situ comparison of Clark and voltammetric electrodes for the determination of O_2. The Mn^{2+} and Fe^{2+} data from voltammetry are also plotted and show no overlap of O_2 with Mn^{2+} because there are no detectable redox species between 2 and 15 mm. A PEEK encased electrode was used for analysis on this dive.

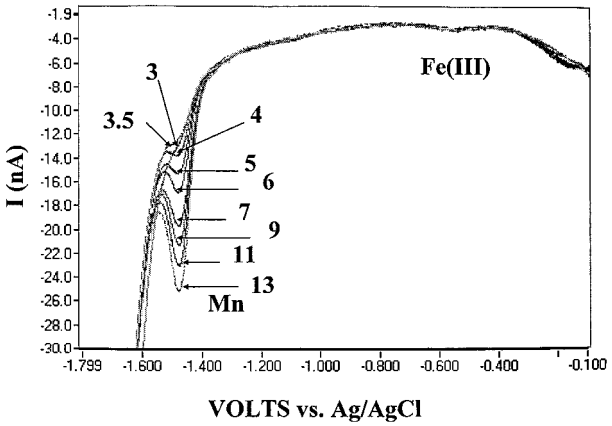

FIGURE 2. In situ voltammetric scans for selected depths obtained for dive 11. The numbers indicate the depth below the water-sediment interface. The traces of Fe(III) are due to organically bound Fe (*12, 13*).

dissolved O_2, Mn^{2+}, and Fe^{2+}. Similar trends for these redox species have been observed for cores brought aboard ship or into the laboratory and analyzed by voltammetry at millimeter vertical resolution (*14*). The difference in the

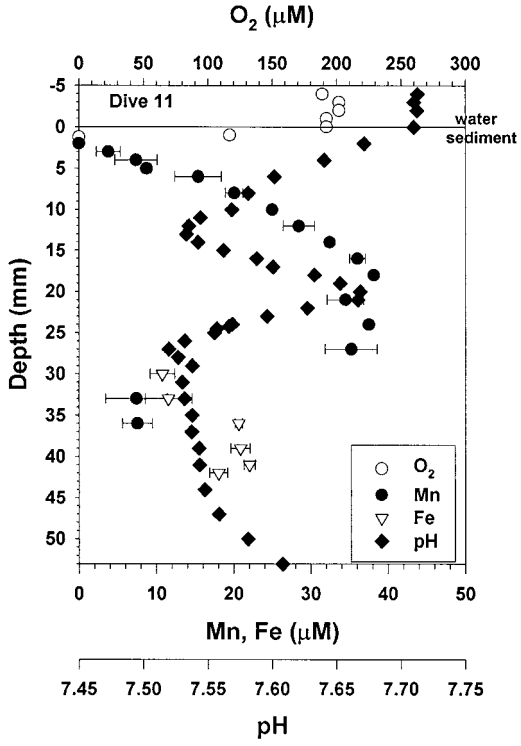

FIGURE 3. Profiles of porewater species measured in real time for dive 11. For this dive and dive 12, glass encased electrodes were used for analysis. The solid-state Au/Hg microelectrode profile was terminated at a depth of 42 mm.

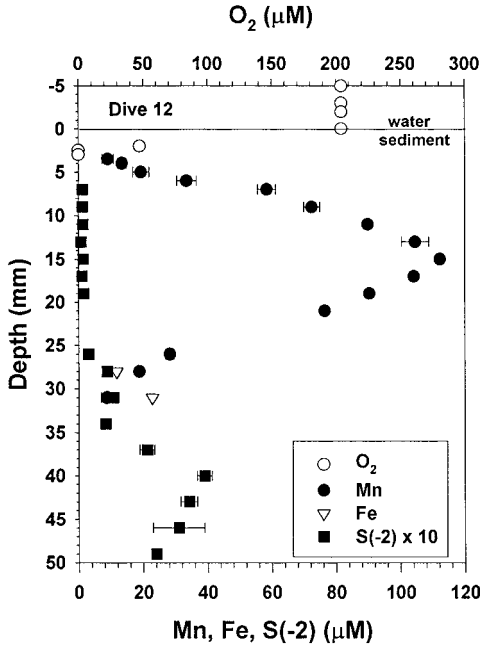

FIGURE 4. Porewater species measured in real time for dive 12; pH data are not available for this dive.

subsurface Mn concentration maximum and the maximum Fe concentration for the different dives is a sign of sediment heterogeneity in the Bay. Sediment heterogeneity and differences in biogeochemical processing of organic matter can be significant as observed in laboratory mesocosm studies *(15)*.

We interpret the pH, O_2, Mn^{2+}, and Fe^{2+} profiles as being determined by organic matter decomposition reactions *(16)* as in eqs 1−5 in conjunction with other secondary reactions between dissolved chemical species:

$$138O_2 + (CH_2O)_{106}(NH_3)_{16}H_3PO_4 \rightarrow 106HCO_3^- + 16NO_3^- + HPO_4^{2-} + 16H_2O + 124H^+ \quad (1)$$

$$94.4NO_3^- + (CH_2O)_{106}(NH_3)_{16}H_3PO_4 \rightarrow 106HCO_3^- + 55.2N_2 + HPO_4^{2-} + 71.2H_2O + 13.6H^+ \quad (2)$$

$$236MnO_2 + (CH_2O)_{106}(NH_3)_{16}H_3PO_4 + 364H^+ \rightarrow 8N_2 + 106HCO_3^- + HPO_4^{2-} + 236Mn^{2+} + 260H_2O \quad (3)$$

$$424FeOOH + (CH_2O)_{106}(NH_3)_{16}H_3PO_4 + 756H^+ \rightarrow 106HCO_3^- + 16NH_4^+ + 424Fe^{2+} + HPO_4^{2-} + 636H_2O \quad (4)$$

$$53SO_4^{2-} + (CH_2O)_{106}(NH_3)_{16}H_3PO_4 \rightarrow 106HCO_3^- + 16NH_4+ + 53HS^- + HPO_4^{2-} + 39H^+ \quad (5)$$

The decrease in pH below the sediment−water interface corresponds to the decrease in O_2 and to a small degree nitrate (bottom water NO_3^- ranged from 6.6 to 6.9 μM). The pH increases from 13 to 21 mm, and the maximum corresponds with the Mn^{2+} increase. The sharpness of the pH profile is consistent with a tightly localized zone of MnO_2 reduction and proton consumption according to eq 3. The decrease in pH and Mn^{2+} below 21 mm appears related to precipitation of carbonate phases which can incorporate Mn and generate $CO_2 + H_2O$ *(4, 17, 18)* or to the adsorption of Mn onto solid phases such as metal carbonates and sulfides *(19)* which are present in the deeper layers of this sediment (data not shown).

Another important point is that O_2 and Mn^{2+} (measured simultaneously with the same voltammetric electrode) did not overlap in any of the profiles based on the minimum detection limits given in Table 1. No detectable O_2 and Mn^{2+} were measured at 2 and 3 mm from dives 11 and 12 (Figures 3 and 4). The profile from dive 6 showed a zone from 2 to 15 mm (data in Figure 1) where no redox species measurable by electrode was present at a concentration above the minimum detection limit. Similar O_2 and Mn^{2+} profiles have been measured aboard ship in sediment cores from the Eastern Canadian continental margin and attributed, in part, to the reduction of NO_3^- to N_2 by Mn^{2+} *(14, 15)*. If little Mn^{2+} is coming into contact with dissolved O_2 via diffusive processes, Mn^{2+} should not be an important contributor to the oxygen flux at this site indicating that $Mn^{2+}$and O_2 are not redox coupled. On the other hand, during episodes of bioturbation or resuspension, dramatic reoxidation of Mn^{2+} by O_2 may be set into play *(18, 20)*.

In addition, the Mn peak at 21 mm (dive 11) and 15 mm (dive 12) is much closer to the surface than those observed in other organic-rich coastal or basin sediment studies *(18, 20−22)*. In these latter studies, traditional cutting and centrifuging of cores were performed with a maximum depth resolution of 2−2.5 mm, and it is possible that mixing of redox species affected the Mn profile including the reaction of Fe^{2+} with MnO_2 to form Mn^{2+} and Fe(III) phases. Microelectrode studies clearly show the separation and variability of redox species as a function of depth in sediments with more detailed resolution and less susceptibility to perturbation of the chemistry of the system than traditional methods. Since such electrode studies are able to be performed in situ, they are also well suited for monitoring seasonal responses of the seafloor to changes in benthic organic matter flux, bioturbation intensity of other natural or anthropogenic disturbances.

Last, for both dives 11 and 12, Fe^{2+} is detected below the Mn^{2+} peak and where Mn^{2+} concentrations approach a minimum. Although Fe^{2+} is readily formed as a result of

microbial reduction as in eq 4, the Fe^{2+} profile appears to be greatly influenced by the formation of iron sulfide solid phases (Figure 3). The chemical and/or biological reduction of Fe(III)−(oxy)hydroxide solid phases results in a pH increase, whereas sulfate reduction (eq 5) and the reaction of Fe^{2+} with HS^- to form FeS both lower pH. Thus, pH changes should not be large (as is observed between 27 and 45 mm) when these reactions occur simultaneously. The small amounts of dissolved sulfide measured for dive 12 indicate that sulfate reduction was occurring in these sediments. Solid-phase analyses of these sediments (data not shown) indicate that both iron monosulfide and pyrite are measurable. Thus, much of the Fe^{2+} formed by reduction of Fe(III) phases was trapped in iron sulfide solid phases which prevented elevated dissolved Fe levels in the porewater.

Conclusions

Real-time measurements of redox species were performed in sedimentary porewaters with voltammetry at a solid-state Au/Hg electrode. A 30 m cable with sender/receiver units allows reproducible signals without deterioration of the signal along the cable for in situ measurements. The profiles of the redox species are consistent with previous profiles obtained aboard ship. These data coupled with pH data indicate that organic matter decomposition by electron acceptors other than O_2 as well as secondary precipitation reactions are mainly responsible for the profiles. The in situ determination of O_2 by Clark-style microelectrodes and voltammetric solid-state electrodes agrees very well. A deployable electrochemical analyzer for in situ voltammetric measurements at any depth in the ocean is under development.

Acknowledgments

This work was funded by grants from the Mid-Atlantic Bight Center of the National Undersea Research Program of the U.S. National Oceanographic and the Atmospheric Administration to C.E.R. and G.W.L. and NOAA Sea Grant program (NA16RG0162-03) to G.W.L. T. Komada, W. Wang, S. Boehme, and A. Bono provided valued assistance.

Literature Cited

(1) Brendel, P. J.; Luther, III, G. W. *Environ. Sci. Technol.* **1995**, *29*, 751−761.
(2) Wang, Y.; Van Cappellen, P. *Geochim. Cosmochim. Acta* **1996**, *60*, 2993−3014.
(3) Reimers, C. E.; Ruttenberg, K. C.; Canfield, D. E.; Christiansen, M. B.; Martin, J. B. *Geochim. Cosmochim. Acta* **1996**, *60*, 4037−4057.
(4) Boudreau, B.; Mucci, A.; Sundby, B.; Luther, III, G. W.; Silverberg, N. *J. Mar Res.* **1998**, *56*, 1259−1284.
(5) Soetaert, K.; Herman, P. M. J.; Middelburg, J. J. *Geochim. Cosmochim. Acta* **1996**, *60*, 1019−1040.
(6) Reimers, C. E. *Deep-Sea Res.* **1987**, *34*, 2019−2035.
(7) Revsbech, N. P.; Jørgensen, B. B. In *Advances in Microbial Ecology*; Marshall, K. C., Ed.; Plenum Press: New York, 1986; Vol. 9, pp 293−352.
(8) Cai, W. J.; Reimers, C. E. *Limnol. Oceanogr.* **1993**, *38*, 1762−1773.
(9) Andrews, D.; Bennett, A. *Geochim. Cosmochim. Acta* **1981**, *45*, 2169−2175.
(10) Skoog, D. A.; Leary, J. J. *Principles of Instrumental analysis*, 4th ed.; Saunders College Publishing: New York, 1992; p 700.
(11) Ewing, G. W. *Instrumental Methods of Chemical Analysis*, 4th ed.; McGraw-Hill Book Co.: New York, 1975; p 560.
(12) Huettel, M.; Ziebis, W.; Forster; S.; Luther, III, G. W. *Geochim. Cosmochim. Acta* **1998**, *62*, 613−631.
(13) Taillefert, M.; Bono, A. B.; Luther, III, G. W. *Environ. Sci. Technol.* Submitted for publication.
(14) Luther, III, G. W.; Sundby, B.; Lewis, B. L.; Brendel, P. J.; Silverberg, N. *Geochim. Cosmochim. Acta* **1997**, *61*, 4043−4052.
(15) Luther, III, G. W.; Brendel, P. J.; Lewis, B. L.; Sundby, B.; Lefrançois, L.; Silverberg, N.; Nuzzio, D. B. *Limnol. Oceanogr.* **1998**, *43*, 325−333.
(16) Froelich, P. N.; Klinkhammer, G. P.; Bender, M. L.; Luedtke, N. A.; Heath, G. R.; Cullen, D.; Dauphin, P.; Hammond, D.; Hartman, B.; Maynard, V. *Geochim. Cosmochim. Acta* **1979**, *43*, 1075−1090.
(17) Mucci, A. *Geochim. Cosmochim. Acta* **1988**, *52*, 1859−1868.
(18) Aller, R. C. *J. Mar. Res.* **1994**, *52*, 259−295.
(19) Arakaki, T.; Morse, J. W. *Geochim. Cosmochim. Acta* **1993**, *57*, 9−15.
(20) Aller, R. C.; Hall, P. O. J.; Rude, P. D.; Aller, J. Y. *Deep Sea Res.* **1998**, *45*, 133−165.
(21) Shaw, T. J.; Gieskes, J. M.; Jahnke; R. A. *Geochim. Cosmochim. Acta* **1990**, *54*, 1233−1246.
(22) Canfield, D. E.; Thamdrup, B.; Hansen, J. W. *Geochim. Cosmochim. Acta* **1993**, *57*, 3867−3883.

Received for review April 30, 1999. Revised manuscript received September 7, 1999. Accepted September 23, 1999.

ES9904991